

Classification
Physics Abstracts
61.16D — 61.70P — 61.80

HREM Observations of Ion Bombardment-Induced Dislocation Loops in ZnO

Jean-Jacques Couderc⁽¹⁾, Jean-Jacques Demai⁽²⁾, Guy Vanderschaeve⁽¹⁾ and Alain Peigney⁽²⁾

⁽¹⁾ Laboratoire de Physique des Solides, ERS CNRS 111, INSA, Complexe Scientifique de Rangueil, 31077 Toulouse Cedex, France

⁽²⁾ Laboratoire de Chimie des Matériaux Inorganiques, ERA CNRS 1311, Université Paul Sabatier, 118 Route de Narbonne, 31062 Toulouse Cedex, France

(Received February 24; accepted April 10, 1995)

Résumé. — On utilise la microscopie électronique en haute résolution pour mettre en évidence des boucles de dislocations partielles provenant de l'amincissement par bombardement ionique d'un échantillon de ZnO. Les défauts d'empilement créés par insertion d'une double couche de Zn-O dans le plan basal sont du type 1Δ .

Abstract. — High resolution electron microscopy (HREM) is used to show faulted dislocation loops resulting from ion bombardment thinning in ZnO. The stacking faults are created by the insertion of a Zn-O double layer in the basal plane and are of the 1Δ type (complex stacking fault).

1. Introduction

High resolution electron microscopy (HREM) investigations of lattice defects in II-VI compounds with the wurtzite structure have already been performed on CdS [1-4], ZnO [5-7] and CdSe strained at room temperature [4]. In the latter material thinned by argon ion milling (beam intensity 250 μ A, accelerating voltage 5kV), interstitial Frank loops were frequently observed; they were considered as having been introduced during the ion thinning process as a result of damage by the ion bombardment.

In the course of a systematic investigation of the microstructure of ZnO-based compounds that are base-constituent of ceramic semiconductor devices (varistors), we have observed that ion bombardment may introduce lattice defects in the thin foil samples. The present paper reports on the results of a HREM study of the irradiation-induced faulted dislocation loops in a doped ZnO crystal with wurtzite structure. The samples have a global cationic composition $Zn_{0.74}Bi_1Mn_1Ti_{0.6}$. They were made by sintering at 950 °C followed by air quenching. Bi and Ti atoms are standard

added elements favouring liquid phase sintering and grain growth, respectively. Mn atoms are added to improve the electrical properties of the compound.

Thin foils suitable for transmission electron microscopy (TEM) were made in the following way: 300 – 400 μm thick slices were cut with a wire saw and then mechanically ground down to 50 μm ; the final thinning was performed by argon ion milling (beam intensity 10 μA , accelerating voltage 6 kV). The preparation of thin samples by chemical methods was unsuccessful.

The observations were carried out on a JEOL 2010 electron microscope operated at 200 kV and fitted with a nanoanalysis EDX equipment (TEM-SCAN service of the Université Paul Sabatier, Toulouse).

2. Stacking Faults in the Wurtzite Structure

A brief description of the wurtzite structure and the different types of stacking faults in this structure is now given.

The wurtzite structure can be represented as a stacking of double layers: aAbBaAbBaAbB (or $\Delta\nabla\Delta\nabla\Delta\nabla\Delta\nabla$ in the Frank notation), packed normal to the [0001] direction. Each layer is composed of one atom species.

Three types of stacking faults are possible in the basal plane:

- i) The intrinsic fault is produced as a result of a slip of a partial Shockley dislocation $1/3 \langle 01\bar{1}0 \rangle$ in the basal plane so that the double layers aA transform into cC, and bB into aA. The faulted sequence is: aAbBaAbBcCaAcCaAcC or $\Delta\nabla\Delta\Delta\Delta\nabla\Delta\nabla\Delta$ (2Δ fault or intrinsic stacking fault according to [4]).
- ii) The extrinsic fault is generated by the insertion of a cC double layer so that the stacking sequence is: aAbBaAbBcCaAbBaAbB or $\Delta\nabla\Delta\nabla\Delta\Delta\Delta\nabla\Delta\nabla$ (3Δ fault or extrinsic stacking fault). It is bounded by a pure Frank partial dislocation $b = 1/2[0001]$.
- iii) The 1Δ fault (or complex fault according to [4]) corresponds to the following stacking sequence: aAbBaAbBcCbBcCbBcC or $\Delta\nabla\Delta\Delta\nabla\Delta\nabla\Delta\nabla$. As shown in [8], it can be produced either by growth, or by a two-stage mechanism (interstitial defect):
 - 1) A two-atom layer is inserted into the cC-position, creating an extrinsic fault bounded by a loop whose Burgers vector is $1/2[0001]$.
 - 2) The loop is swept by a single Shockley partial ($b = 1/3 \langle 01\bar{1}0 \rangle$) leaving a complex fault with displacement vector $\mathbf{R} = 1/2[0001] + 1/3 \langle 01\bar{1}0 \rangle = 1/6 \langle 02\bar{2}3 \rangle$. The 3Δ stacking fault is transformed into a single 1Δ complex fault. A similar mechanism is involved for the generation of 1Δ vacancy loops.

Notice that both 1Δ and 3Δ faults are bounded by dislocation loops whose Burgers vectors ($1/6 \langle 02\bar{2}3 \rangle$ and $1/2[0001]$ respectively) do not lie in the fault plane. The Burgers vector lengths are in the ratio $(c^2/4 + a^2/3)^{1/2} / (c/2)$, i.e. 1.23 in the case of ZnO ($a = 0.3249 \text{ nm}$, $c = 0.52047 \text{ nm}$).

The relative energies of the various types of stacking faults are expected to be roughly proportional to the number of wrong second neighbour stackings; therefore the approximative stacking fault energy ratio is $1/2/3$ for the 1Δ , 2Δ and 3Δ stacking faults, respectively. Consistent with this view, in CdSe [4], interstitial type Frank loops were frequently observed to nucleate on wide intrinsic stacking faults generated by plastic deformation, thus transforming a 2Δ fault into a 1Δ one.

3. Observations

Conventional TEM observations revealed the presence of both intergranular micrometric phases (β -Bi₂O₃ and Zn₂TiO₄) and intragranular nanometric precipitates (including Mn and Ti atoms) [9]. In the course of a HREM investigation which was primarily intended to study the structure and coherency of the latter ones, faulted loops, whose diameter ranges from 3 to 12 nm were observed. They are viewed edge-on in Figure 1 and appear as fine dark or light lines. The density of loops is very high in the thinnest part of the foil (about 10¹⁴⁻¹⁵/mm³). So small features were hardly distinguished using conventional dark field techniques, owing to the surface damage due to ion beam thinning. On the other hand EDX analysis (probe size 1.5 nm) inside the loops did not reveal the presence of any impurities. So it is likely that the loops do not result from any segregation of Bi, Mn and Ti doping atoms.



Fig. 1. — Lattice image taken with the ± 0001 , ± 0002 diffracted waves of an area with a high density of faulted loops. The electron beam is parallel to $[2\bar{1}\bar{1}0]$. The spacing of the lattice fringes (0.52 nm) corresponds to the interplanar distances between basal planes (d_{0001}).

Figure 2 shows an area free from defects: the HREM image consists of rows of white spots that are slightly in zig-zag in the c direction. As shown in [3] each bright spot corresponds to a close pair of zinc and oxygen atomic rows.

Figure 3 shows an insertion dislocation loop. One can see that the aAbB stacking of the wurtzite structure is modified into aAbBaAbBcCbBcCbBcC ($\Delta\nabla\Delta\nabla\Delta\Delta\nabla\Delta$), that is a 1Δ stacking fault,

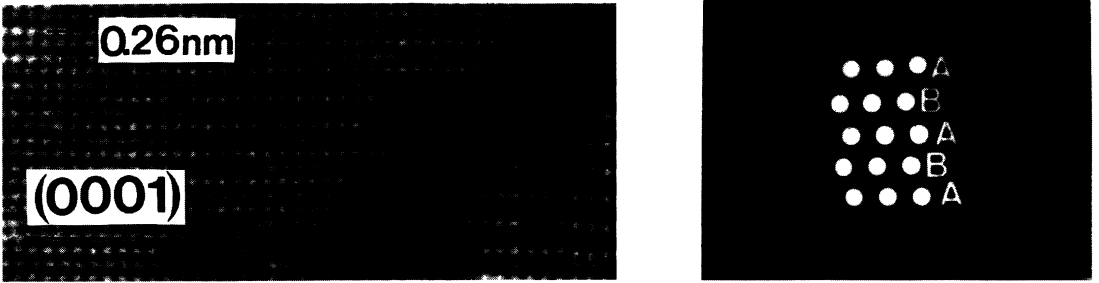


Fig. 2. — a) HREM micrograph of an area free from defects taken with the electron beam parallel to $[21\bar{1}0]$ using 16 diffracted waves. b) Schematic representation of the stacking sequence in the $[0001]$ direction.

the partial dislocations that limit the fault on both side having $b = 1/6 \langle 02\bar{2}3 \rangle$. All the faulted loops investigated were found to be of the same type.

4. Discussion

As mentioned above, the presence of these defects cannot be attributed to the segregation of Mn, Bi, Ti impurities. It is suggested that the insertion loops have probably been produced during the ion bombardment that would promote a migration and a condensation of interstitial atoms (both Zn and O).

The following discussion will focus on two main points of the present study: the occurrence of 1Δ loops and a comparison in the defect structure resulting from either ion bombardment or electron irradiation.

4.1 WHY ARE ONLY 1Δ LOOPS OBSERVED?. — In our experiments only 1Δ faulted loops were observed. As mentioned above, these defects are generated firstly by inserting a double layer of Zn and O interstitial atoms and subsequently transforming the so-created 3Δ fault into a lower energy 1Δ one by nucleation of a Shockley partial loop. At first sight, the present observations could be accounted for by comparing the relative energies of 1Δ and 3Δ stacking faults. Nevertheless, assuming the defects (1Δ and 3Δ faulted loops) are in their equilibrium configuration, a discussion of their relative stability should compare their total energy, which includes both the surface energy of the stacking faults and the line energy of the dislocation loops. Calculations (see appendix) indicate that if $\gamma_{3\Delta} - \gamma_{1\Delta}$, which is roughly equal to $\gamma_{2\Delta}$ (γ : Stacking fault energy), is higher than a critical value γ_c , 1Δ loops are stable whatever their size; if $\gamma_{3\Delta} - \gamma_{1\Delta}$ is lower than γ_c only loops with radius r lower than a critical value r_c are stable in their 3Δ form. Note that both γ_c and r_c strongly depend on the core radius chosen in the calculation; γ_c is certainly higher than 370 mJ/m^2 . Unfortunately, the fault energies in ZnO are not precisely known so that no definite conclusions can be drawn. Consistent with the previous results of Takeuchi *et al.* [10], we were not able to observe dissociated perfect dislocations in this compound, even when using dark field weak beam imaging. Accordingly, only a lower limit of $\gamma_{2\Delta}$ can be estimated: $\gamma_{2\Delta} > 43 \text{ mJ/m}^2$ [10].

It was previously shown that ion bombardment induced the formation of 1Δ and 3Δ faults in CdSe with wurtzite structure [4]. As mentioned above, 1Δ faults were observed to form by nucleation of Frank loops on preexisting glide stacking faults. Apparently, in the specimen areas free from wide intrinsic stacking faults, only 3Δ faulted loops were observed, at variance with

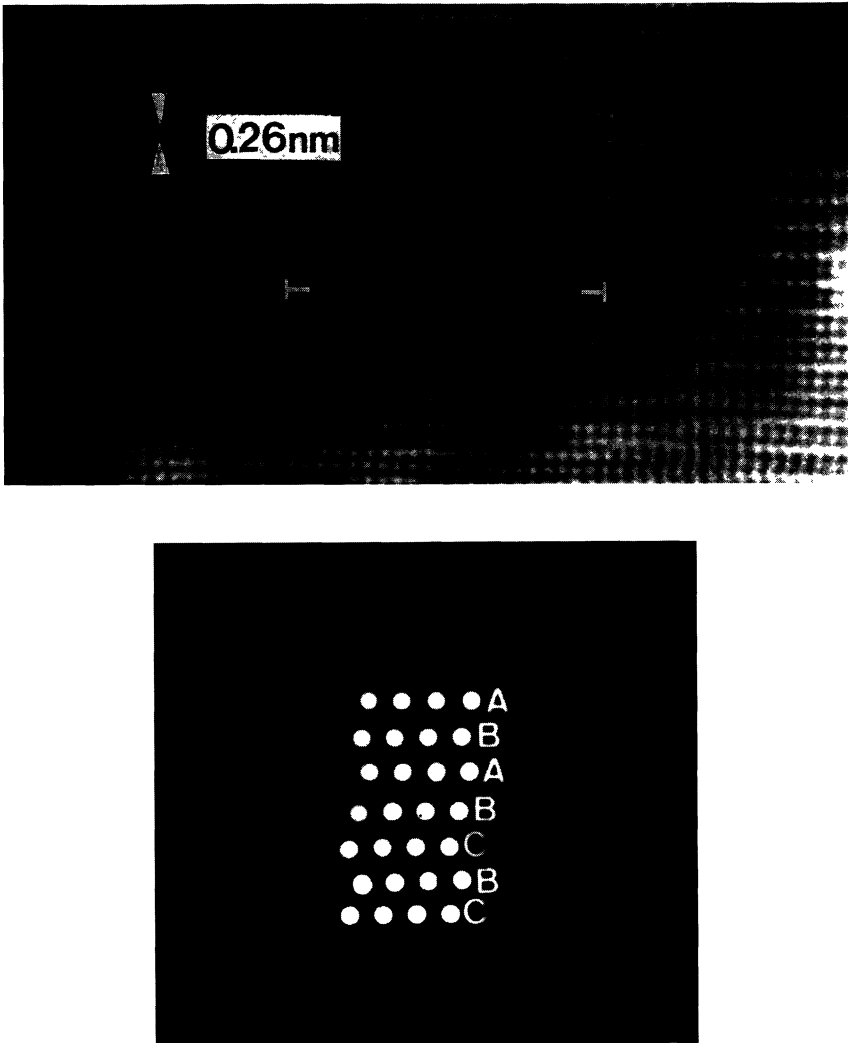


Fig. 3. — a) HREM image of a complex 1Δ fault (same conditions as Fig. 2a). b) Schematic representation of the stacking sequence of a 1Δ stacking fault.

the present results in ZnO. This could be related to the rather low value of $\gamma_{2\Delta}$ in CdSe: $\gamma_{2\Delta} = 14 \pm 5 \text{ mJ/m}^2$ [4, 10].

4.2 COMPARISON WITH ELECTRON IRRADIATION EXPERIMENTS. — Another way to produce interstitial extended defects in ZnO is electron irradiation with a high voltage electron microscope. It has been shown elsewhere that dislocation loops nucleate both on preexisting stacking fault planes and in regions free from stacking faults as a result of irradiation with 700 keV electrons. In the latter regions two types of interstitial loops were identified: perfect loops lying in the prismatic planes and 3Δ faulted loops lying in the basal plane. No 1Δ faulted loops were observed in these regions [11-14].

The difference in the defect structure of ZnO resulting from either ion bombardment (present work) or high energy electron irradiation [11-14] is not fully understood. According to Yoshiie *et al.* [13-14], the loop nucleation process in semiconducting crystals is an heterogeneous process with some special site (impurity atoms, defect clusters) as the nucleation site of the crystal. The nature and efficiency of the nucleation site may depend on:

- i) The nature of the incident particle: according to [15], charged particle damage (high transmitted energy, low particle flux) is characterized by a small number of large disordered regions superimposed upon a larger relative number of small clusters of defects, whereas almost all primary damage due to electron irradiation (low transmitted energy, high electron flux) is in the form of single interstitial vacancy pairs.
- ii) The purity of the material: the material used in the electron irradiation experiments was ZnO films prepared in the form of ribbons thin enough for electron microscope observations, by hydrolytic reaction of ZnS vapor at 1100 °C [13-14]. The material used in the present investigation was bulk doped ZnO.
- iii) The irradiation temperature.
- iv) The diffusion processes which are certainly different in thin films and in bulk crystals.

Finally, one cannot exclude the possibility that the 1Δ loops observed after Ar ion bombardment are not in the equilibrium configuration.

Appendix

On the Relative Stability of 1Δ and 3Δ Faulted Loops

The total energy of a faulted loop includes both the elastic self energy of the dislocation loop W_1 and the surface energy of the enclosed stacking fault (S.F.). For a 3Δ faulted loop of radius r (Burgers vector $c/2 = 1/2[0001]$ normal to the fault plane) it may be written as:

$$W_{3\Delta} = \pi r^2 \gamma_{3\Delta} + W_1(c/2)$$

where $\gamma_{3\Delta}$ is the S.F. energy of the 3Δ fault and $W_1(c/2)$, the self energy of the corresponding Frank loop.

Sweeping the 3Δ faulted loop by a glissile Shockley partial (Burgers vector $p = 1/3\langle 01\bar{1}0 \rangle$) leads to the formation of 1Δ faulted loop, whose energy is then:

$$W_{1\Delta} = \pi r^2 \gamma_{1\Delta} + W_1(c/2) + W_1(p)$$

where $\gamma_{1\Delta}$ is the S.F. energy of the 1Δ fault and $W_1(p)$ is the self energy of the Shockley loop.

In writing this expression, it is implicitly assumed that there is no elastic interaction between the Frank and Shockley loops, which is certainly a correct approximation since their Burgers vectors are perpendicular.

Then the relative stability of both faulted loops depends on the difference

$$W_{3\Delta} - W_{1\Delta} = \pi r^2 (\gamma_{3\Delta} - \gamma_{1\Delta}) - W_1(p)$$

In the frame of the isotropic elasticity, the self energy of a glissile loop with Burgers vector p may be written [16]:

$$W_1(p) = 2\pi r \mu [1 + 1/(1 - \nu)] (p^2/8\pi) \ln [(4r/\rho) - 2]$$

with μ : shear modulus, ν : Poisson ratio, ρ : core parameter.

However, hexagonal crystals are isotropic in the basal plane. This makes it possible to take anisotropy into account in the calculations. As shown by Hirth and Lothe [16], the energy expression of the isotropic theory is correct with a particular choice for μ and $\mu/(1-\nu)$; $\mu = K_s$, $\mu/(1-\nu) = K_e$, where K_s and K_e depend on the elastic constants of the material. So, in the frame of the anisotropic elasticity theory, $W_1(p)$ may be written as ($p = a/\sqrt{3}$, a : lattice parameter):

$$W_1(p) = (a^2 r/12) (K_e + K_s) \ln(4r/\rho - 2)$$

Introducing $W(R) = (W_{3\Delta} - W_{1\Delta})/\pi a^3$, one has

$$W(R) = \Gamma R^2 - \alpha R \ln \beta R, \text{ where } R = r/a.$$

$\Gamma = (\gamma_{3\Delta} - \gamma_{1\Delta})/a$ depends on the S.F. energies

$\alpha = (K_e + K_s)/12\pi$ depends on the elastic constants of the material

$\beta = 4a/\rho e^2$ (e : basis of neperian logarithms), depends on the dislocation core radius.

Calculations indicate that:

- i) when $\Gamma > \Gamma_c = \alpha\beta/e$, $W(R)$ is always > 0 , that is the 1Δ faulted loop is always stable.
- ii) when $\Gamma < \Gamma_c$, only loops with R greater than a critical value R_c (for which $W(R_c) = 0$) are stable in their 1Δ form ($W(R > R_c) > 0$).

For ZnO, $a = 0.3249$ nm, $K_s = 4.34 \cdot 10^{10}$ N/m² and $K_e = 7.26 \cdot 10^{10}$ N/m² (these values being calculated from the elastic constants given in [17]) and $(\gamma_{3\Delta} - \gamma_{1\Delta})_c = \gamma_c = a\Gamma_c = 370\beta$ (mJ/m²).

It is seen that γ_c strongly depends on the core parameter, the correct value of which is still debated. A lower limit of β is certainly $\beta = 1$, so that $\gamma_c > 370$ mJ/m². For lower values of $(\gamma_{3\Delta} - \gamma_{1\Delta})$, the stability of the loops depends on their size. As an example, for $(\gamma_{3\Delta} - \gamma_{1\Delta}) = 100$ mJ/m², the critical radius $r_c = aR_c$ above which 1Δ loops are energetically stable is (with $\beta = 1$) $r_c = 12$ nm.

References

- [1] Sinclair R., Ponce F.A., Bravman J.C., Yamashita T. and Pirouz P., in: "Microscopy of Semiconducting Materials", A.G. Cullis and D.C. Joy Eds. (The Inst. Phys. Bristol and London, 1981) 147.
- [2] Yamashita T., Ponce F.A., Pirouz P. and Sinclair R., *Philos. Mag. A* **45** (1983) 693.
- [3] Echigoya J., Pirouz P. and Edington J.W., *Philos. Mag. A* **45** (1982) 455.
- [4] Suzuki K., Takeuchi J., Shino M., Kanaya K. and Iwanaga H., *Techn. Report of ISSP Ser. A* (1983) N° 1304.
- [5] Clarke D.R., *J. Appl. Phys.* **49** (1978) 2407.
- [6] Suyama Y., Tomokiyo Y., Manabe T. and Tanka E., *J. Am. Ceram. Soc.* **71** (1988) 391.
- [7] Jong Choul Kim and Goo E.J., *Am. Ceram. Soc.* **73** (1990) 877.
- [8] Amelinckx S., "Dislocations in particular structures", in *Dislocations in Solids*, Vol. 2, F.R.N. Nabarro Ed. (North-Holland Publishing Co, 1982) 171.
- [9] Peigney A., Couderc J.J., Demai J.J., Carles V. and Rousset A., *Electron Microscopy 1994, ICEM-13* (Ed. de Physique, Paris, 1994) 847.
- [10] Takeuchi S., Suzuki K. and Maeda K., *Philos. Mag. A* (1984) 171.
- [11] Iwanaga H., Suzuki K. and Takeuchi S., *Philos. Mag.* **34** (1976) 291.
- [12] Iwanaga H., Shibata N., Suzuki K. and Takeuchi S., *Philos. Mag.* **35** (1977) 1213.
- [13] Yoshiie T., Iwanaga H., Shibata N., Suzuki K., Ichihara M. and Takeuchi S., *Philos. Mag. A* **47** (1983) 315.
- [14] Yoshiie T., Iwanaga H., Shibata N., Suzuki K. and Takeuchi S., *Philos. Mag. A* **41** (1980) 935.
- [15] Crawford J.H., *The Interaction of Radiation With Solids*, R. Strumane, J. Nihoul, R. Gevers and S. Amelinckx Eds. (North Holland, Amsterdam, 1964) 421.
- [16] Hirth J.P. and Lothe J., *Theory of Dislocations* (McGraw-Hill, N.Y., 1968).
- [17] Bateman T.B., *J. Appl. Phys.* **33** (1962) 3309.